

# SURFACE LAYER'S SOUND SPEED PROFILES: CLIMATOLOGICAL ANALYSIS AND APPLICATION FOR THE CNOSSOS-EU NOISE MODEL

Tamás Weidinger<sup>1\*</sup>, Edina Balogh<sup>2</sup>, Abderrahmane Mendyl<sup>1</sup>, Petra Fritz<sup>1</sup>, Ágoston Vilmos Tordai<sup>1</sup>, Arun Gandhi<sup>1</sup>, and Tamás Schmelz<sup>2</sup>.

<sup>1</sup>Eötvös Loránd University Faculty of Sciences, Institute of Geography and Earth Sciences, Department of Meteorology, Pázmány Péter sétány 1/A, H-1117, Budapest, Hungary

<sup>2</sup>KTI Institute for Transport Sciences Non-profit Ltd., Research Centre for Sustainable Transport, Department for Transport Acoustics, 3-5 Than Károly street, H-1119, Budapest, Hungary

**Abstract:** Noise pollution and exposure are important environmental issues that need to be investigated and regulated. To do this, we need to know about micrometeorology to figure out how noise travels from the source to the receiver. Accordingly, the sound propagation part of the common noise assessment methods (CNOSSOS-EU) developed by the European Commission for different sources of noise needs detailed meteorological databases. Using data from the SYNOP stations maintained by the Hungarian Meteorological Service (HMS) and the ERA5 meteorological reanalysis database, the standard noise propagation conditions are determined. The primary objective of this study is to ascertain the probability distribution of stability classes for a variety of source-receiver orientations, utilizing either 25 or 2 stability classes, and several different aggregation levels. Relative frequencies and year-to-year variability have been calculated for favourable noise propagation conditions where the sound speed profile grows with height (downward refraction condition) and unfavourable noise propagation conditions where the sound speed profile constant or decreases with height (so-called homogeneous conditions). Favourable noise propagation occurs in approximately one-third of cases during the daytime while in approximately two-third of cases during the evening and night-time where the noise exposure is increasing. Furthermore, using the SoundPLANnoise software, sound propagation model calculations were performed on a study area near Budapest, using different values of parameter  $p_f$  describing the probability of occurrence of favourable conditions on sound propagation during different periods of the day. This area is crossed by Highway 4, which is a major road according to the 49/2002 EU Directive, as it has more than three million vehicles passing on the examined section every year. The results show considerable deviations in annual average A-weighted sound levels calculated using different versions of parameter  $p_f$ . The largest difference between the A-weighted sound levels calculated with the highest and lowest generated annual  $p_f$  values was 1.65 dB(A); 1.42 dB(A) and 0.75 dB(A) for day, evening and night periods, respectively.

**Keywords:** CNOSSOS-EU, ERA5, meteorological preprocessor, noise model, SoundPLANnoise software

## 1 INTRODUCTION

The noise pollution load from transportation, industrial production, entertainment, and concerts is substantial, making an investigation of atmospheric sound propagation realistically vital. In sound propagation modelling, there are different types of point, line, and areal sources (Deepak, 2016; Guski et al., 2017). We concentrate only on the point sources. Sound levels between 30-90 dB(A) are the most common in everyday life, and they are especially bothersome at night. Approximately 20% of the European population is subject to long-term excessive noise exposure which is harmful to their health (Peris, 2020). According to the World Health Organisation (WHO), noise is the second most common environmental cause of health problems, just after particulate matter (PM). According to the Budapest Environmental Condition Assessment prepared by the Municipality of Budapest – Budapest City Urban Planning Ltd. in 2022, about 27% of the population in Budapest was exposed to a noise level above 65 dB(A) for the  $L_{den}$  noise indicator in 2017, which can already be considered harmful to health ( $L_{den}$  is the annual day-evening-night noise level based on energy equivalent noise level ( $L_{eq}$ ) over a whole day with a penalty of 10 dB(A) for night time noise (22.00-06.00 h in legal time) and an additional penalty of 5 dB(A) for evening noise (18.00-22.00 h)). The difference between night-time and daytime noise level was only 4-7 dB(A) on average, which means that even at night the noise exposure is significant. Data from 2017 also shows that 38.2% of population in Budapest was exposed to road traffic noise levels above 55 dB(A)  $L_{den}$  (Khomenko et al., 2022). This is a quite high rate, considering the WHO recommendation that road traffic noise levels should be reduced below 53 decibels  $L_{den}$  to avoid adverse health effects (WHO, 2018).

To avoid, prevent or reduce the harmful effects due to exposure to environmental noise, EU Member States are required to prepare strategic noise maps and action plans for agglomerations (urbanized areas with more than 100,000 inhabitants), and also for major roads, major railways and major airports every five years as covered in Directive 2002/49/EC (2002). The Member States determined the limit values of each noise indicator to be calculated as day-evening-night noise indicator  $L_{day}$  [dB(A)]

and night-time noise indicator  $L_{night}$  [dB(A)] for different types of noise. If the values of the calculated noise indicators exceed the limit values, mitigation measures are to be considered. In Hungary, the limit values for industrial sources are 46 dB(A) and 40 dB(A) for overall annoyance and night-time, respectively. Regarding the traffic sources, limit values are  $L_{day} = 63$  dB(A) and  $L_{night} = 55$  dB(A) according to the Hungarian legislation.

To harmonize the methods used to calculate, predict, estimate or measure the value of a noise indicator or the related harmful effects, a common assessment method was developed and published in the Commission Directive (EU) 2015/99 (Directive 2015/996/EU, 2015). To prepare the strategic noise maps, Member States are required to use the new common assessment method (CNOSSOS-EU method) from 31 December 2018 onwards. On the other hand, determining the input data of the model calculation (e.g. traffic flow data, meteorological data) may require measurements, if the default values specified in the CNOSSOS-EU Directive (Directive 2015/996/EU, 2015) are not applicable. Furthermore, there are input data for which the Directive does not specify default values at all (e.g.  $p_f$  parameter). The determination of these input data may also require measurements.

The noise propagation model of the CNOSSOS-EU method requires a detailed meteorological database for the calculation of the sound speed profiles between the source and the receiver (or so called receptor) point (Eurasto, 2006; Defrance et al., 2007; Majjala and Kontkanen, 2016).

The task is to determine the probability ( $p_f$  [%]) of these downward refraction (increasing with height) vertical sound speed profiles and the probability ( $1-p_f$  [%]) of homogeneous noise propagation vertical sound profiles during 3 time periods – night, day and evening. The calculations are provided based on the hourly measurements of temperature, atmospheric stability, wind speed, and direction at different periods of the day based on the surface meteorological data and source-receiver directions using 5-10 years of time series. It should be pointed out that in our model only sound sources close to the ground and noise propagation in the surface layer (max. 100 m above the ground) are considered. The results cannot be used for higher sound sources, e.g. wind energy turbines.

After an overview of the theoretical background of noise propagation, the role of the different atmospheric stability classes is described. Calculations of the Pasquill-Gifford stability classes and the generation of near-surface sound speed profiles are also presented based on the calculation of wind speed and acoustic virtual temperature profiles using the Monin-Obukhov similarity theory (Foken, 2017). Based on the methodology, firstly 25 types of stability and wind speed-dependent sound speed profiles are used (Defrance et al., 2007).

The Hungarian meteorological preprocessor developed for the noise propagation model of the CNOSSOS-EU method is also provided. The probability of occurrence of downward refraction conditions ( $p_f$ ) is presented based on ten years of hourly SYNOP observations from the György Marczell Main Observatory of the HMS (Budapest, 12843). Three parts of the day are investigated separately: the night period (22.00-06-00 h – in legal (or normal) time in Hungary with the change between summer and winter time), the day period (06.00-18-00 h) and the evening period (18.00-22-00 h). Differences among years are also analysed. Results obtained from five additional weather stations with a 5-year long time series are also presented. Finally, the comparison of results ( $p_f$ ) from the measured and the ERA5 reanalysis dataset (Hersbach et al., 2020) for Budapest was provided. The ERA5 reanalysis database – together with the meteorological variables – contains the radiation balance components (short- and longwave) and the surface energy budget components, such as momentum, sensible and latent heat fluxes, friction velocity ( $u_*$  [m/s]), temperature scale ( $T_*$  [K]), and Monin-Obukhov length ( $L_*$  [m]) (Arya, 2001; Foken, 2017). The occurrence of downward refraction conditions ( $p_f$ ) is calculated based on the meteorological variables and directly from the surface layer turbulence characteristics.

Based on generated  $p_f$  values, sound propagation model calculations were also performed on a study area, located along a major road in Hungary. In addition to  $p_f$  values calculated based on 10-year observations for the region of Budapest using hourly SYNOP dataset from Pestszentlőrinc weather station (12843), other versions of parameter  $p_f$  were also used as input data (e.g.  $p_f = 1$  as worst case-scenario). Sound levels for each period of day (day, evening and night period) were calculated at receiver points designated in increasing distance from the source. Sound levels resulted from different values of the parameter  $p_f$  were compared to each other to examine the effect of the accuracy of the parameter  $p_f$  on CNOSSOS-EU sound propagation model outputs.

## 2 MATERIAL AND METHODS

### 2.1 SOUND SPEED PROPAGATION

Sound waves are density waves. The equation of propagation  $c_{ad}$  [m/s] adiabatic sound speed in moist air with pressure  $p$  [Pa], temperature  $T$  [K] and water vapour pressure  $e$  [Pa] is:

$$c_{ad} = \sqrt{k_m R_m T_m} = \sqrt{k_m R_d T_v} = \sqrt{k R_d T_{av}} \quad (1)$$

where  $k = c_{p_m}/c_{v_m} \approx k * (1 - 0.1q)$  is the ratio of the specific heat capacity for moist air (lower index  $m$ ) at constant pressure and constant volume, where  $k = c_{p_d}/c_{v_d}$  is equal to the ratio of the specific heat capacities for dry air (lower index  $d$ )  $k = 1.4$  (Tsonis, 2007; Fiorino et al., 2021),  $R_d = 287$  J/kg K is the specific gas constant for the dry air,  $T_{av}$  [K], is the acoustic virtual temperature (Ostashev and Wilson, 2015).

$$T_{av} = T(1 + 0.511q) \quad (2)$$

where the specific humidity ( $q$  [kg/kg]) is the ratio of the water vapour density and the wet air density (Ostashev and Wilson, 2015; Foken, 2017):

$$q = 0.622 \frac{e}{p - 0.378e} \quad (3)$$

The acoustic virtual temperature ( $T_{av}$ ) is close to the virtual temperature used in the meteorology ( $T_v = T(1 + 0.608q)$ ). If the sound travels from a more acoustically dense” medium with a lower propagation speed (e.g., a lower temperature) to a „less acoustically dense” medium, it will be refracted (Figure 1a, b). The propagation speed of the wave increases as it enters the acoustically less dense medium. The direction of sound propagation and the angle of refraction of the sound wave at the boundary of the two media (the angle subtended by the normal of the surface) are also changed. The ratio of the sine of the two angles is equal to the ratio of the speed of sound in the two media. This is the well-known Snellius-Descartes law, in wave theory (Garrett, 2020). The speed of sound decreases with height during daytime and increases at night (inversion) due to stable stratification. It is true for average conditions and especially for weather patterns that develop from local conditions (without passage of weather fronts and low pressure areas (in calmly situations)) (Fig. 1a,b).

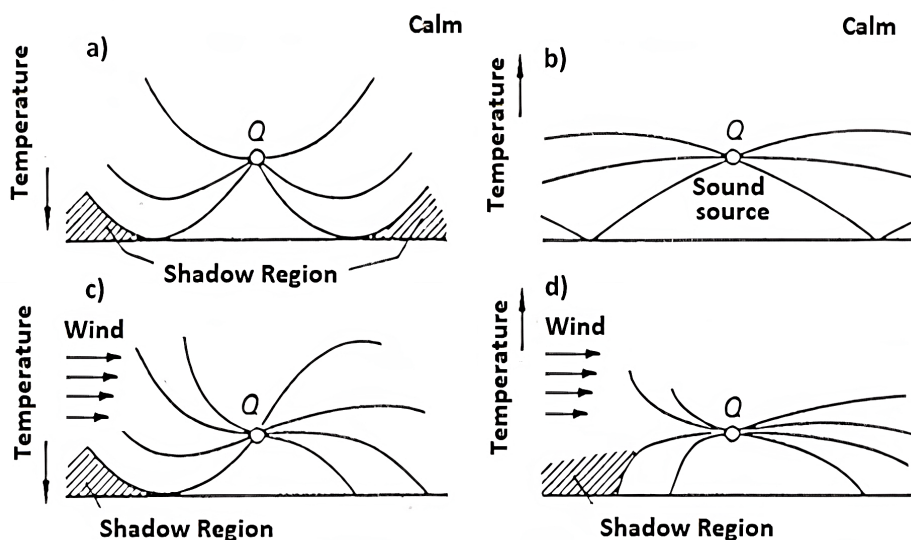


Fig. 1: Sound propagation (along curved paths due to refraction) as a function of temperature stratification during calm periods for unstable (a) and stable (b) stratification, with wind profile modification (c, d) (after Foken, 2017) (VDI, 1988, published with kind permission of © VDI e.V. and Beuth-Verlag Berlin 1988, and Foken (2017), All rights reserved).

The noise propagation is modified by the relative wind speed (upwind, crosswind, and downwind) depending on the source-receiver position. Downwind is blowing from the noise source to the receiver point in the direction of the sound propagation and increasing it (Fig. 1c, d). Note that the total crosswind (the wind vector perpendicular to the line of the source-receiver points) has no effect on the sound propagation. Upwind is blowing from the receiver point to the noise source in the opposite direction of the sound propagation and decreasing it.

Thus, the speed of sound propagation depends on i) the wind speed profile ( $V(z)$ ), ii) the direction of sound propagation, iii) the angle  $\varphi$  between the point source and the wind flag (Fig. 2), as seen from the receiver point in the “centre of the circle”, and iv) the temperature changes with height. In a full downwind, the wind blows from the noise source to the receptor point. The angle between the actual wind direction (the wind flag) and the noise source is then  $\varphi = 0^\circ$ , while  $\varphi = 180^\circ$  for upwind and  $\varphi = 90^\circ$  or  $\varphi = 270^\circ$  for full crosswinds. (In meteorology, the current wind direction is the direction from which the wind blows always on horizontal plane.) The wind develops or strengthens the shadow zone on the upstream side (wind blowing from the receptor point towards the sound source); while on the downstream side, the wind weakens or dissipates the shadow zone, increasing the noise exposure. Note that for the presented surface layer approaches in the CNOSSOS-EU model, several assumptions are made, including horizontal homogeneity of meteorological fields and vegetation/surface properties with given roughness length (Arya, 2001; Attenborough, 2014; Foken, 2017). We assume the constant surface flux layer with horizontally homogeneous and isotropic turbulence regime where the wind direction does not change with height. Monin-Obukhov similarity theory was applied where the wind speed always increases with height in the surface layer. For indifferent stratification, we use a logarithmic profile approximation. In the case of unstable stratification, the wind speed increases less than logarithmically with height, while in stable stratification it increases more than logarithmically (Foken, 2017). We also used the stability dependent monotone temperature profiles based on Defrance et al. (2007) and Attenborough (2014).

These provide the meteorological background of the modelling based on the long-term meteorological station and reanalysis datasets. This is complemented by information on topography, land cover, soil condition, etc. in the noise propagation calculations for a given location based on the requirements of CNOSSOS-EU model approaches (Faulkner et al., 2021; Balogh et al., 2022). Our goal is creating a noise propagation meteorological preprocessor providing general-purpose as regional background dataset. Thus, the next step is the preparation of wind speed, temperature and sound speed profiles in the surface (constant flux) layer.

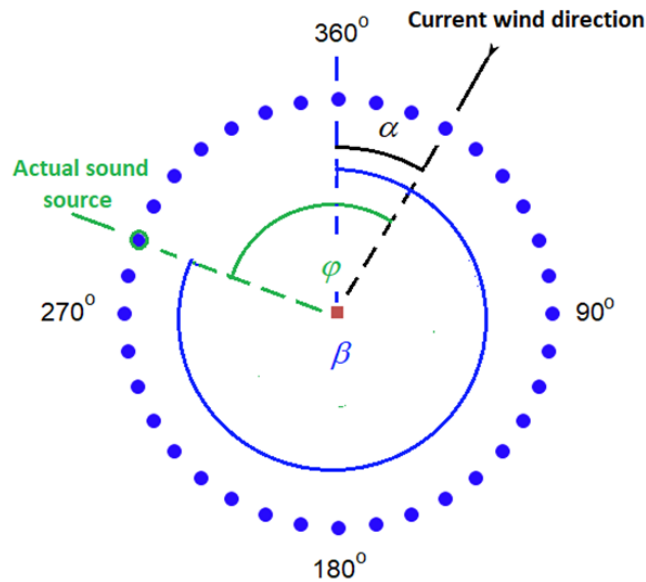


Fig. 2: Source-receptor relationships. For a given wind direction  $\alpha$ , the hypothetical noise sources are positioned at every 10 degrees and the angle  $\varphi$  is subtended by the wind flag” (actual wind direction) as seen from the receptor point. The hypothetical noise sources are indicated by the blue circles and the receptor point by the red rectangle.  $\beta$  corresponds to the position of the actual noise source. Propagation categories (homogeneous or downward refraction) are given for the 36 hypothetical sources in each hour. This is a typical crosswind situation between the actual noise source (green) and the receiver point (red).

## 2.2 Sound speed profiles

The variation of the sound speed with height depends on the wind speed and acoustic virtual temperature profiles and the angle between the current noise source and the wind direction (Fig. 2). Log-linear profile approximations were used for stable and unstable stratifications with different constants, obtained by integrating the simplified universal functions of the Monin-Obukhov similarity theory (Weidinger et al., 2000; Arya, 2001). The shapes of the commonly used sound speed profiles are in cf. e.g. Eurasto (2006), Defrance et al. (2007), Dutilleux et al. (2009) and Attenborough (2014):

$$c(z) = c_{ad}(z) + u(z) = a \ln\left(1 + \frac{z}{z_0}\right) + bz + c_0 \quad (4)$$

$$c_{ad}(z) \approx c_0 + \frac{1}{2} \frac{kR_d}{c_0} (T_{av}(z) - T_{av0}) \approx c_0 + a_c \ln\left(1 + \frac{z}{z_0}\right) + b_c z \quad (5)$$

$$u(z) = V(z) \cos \varphi \approx a_u \ln\left(1 + \frac{z}{z_0}\right) + b_u z \quad (6)$$

with

$$a = a_u + a_c, b = b_u + b_c \quad (7)$$

where  $a$  [m/s] is constant of logarithmic term in sound speed profile,  $a_c$  [m/s] is constant of logarithmic term in acoustic virtual temperature profile,  $a_u$  [m/s] is constant of logarithmic term in wind speed profile,  $b$  [1/s] is constant of linear term in sound speed profile,  $b_c$  [1/s] constant of linear term in acoustic virtual temperature profile,  $b_u$  [1/s] constant of linear term in wind speed profile. In the equations (4-7) are the variables:  $c$  [m/s] is the sound speed in the atmosphere in  $z$  [m] height above the surface,  $V$  [m/s] wind speed,  $u$  [m/s] effective wind speed for calculation of noise propagation in  $z$  height,  $c_0$  [m/s] sound speed near the surface,  $T_{av0}$  [K] reference acoustic virtual temperature near the surface,  $z_0$  [m] roughness length which is 0.1 m in our cases. The effective wind speed  $u(z)$  at any height  $z$  is defined in equation (6) as  $u(z) = V(z) \cos \varphi$ . By this definition, effective wind speed  $u(z)$  is that component of the horizontal wind speed  $V(z)$  which is parallel to the line connecting the source of sound and the receptor point. It is the reason why cross winds which are perpendicular to the line joining noise source and receptor point does not have any effect on the sound propagation as  $\cos \frac{\pi}{2}$  or  $\cos \frac{3\pi}{2} = 0$ .

The constants in the equations are defined as a function of the atmospheric stability using the Pasquill-Gifford stability categories (Mohan and Siddiqui, 1998), following the methodology of Eurasto (2006), Defrance et al. (2007) and Dutilleux et al. (2009). The hourly synoptic datasets of Hungarian Meteorological Service (HMS) were downloaded from the Meteomanz and Ogimet websites

for those years when cloud measurements were available. The meteorological variables of synoptic meteorological (SYNOP) stations present in the dataset are temperature [°C] and relative humidity [%] in 2-m height, pressure [hPa], wind speed [m/s] and wind direction [degrees] in 10-m standard level with 10 min average time and cloudiness [Octa]. The amount of cloud cover is given in octas (0, 1, ..., 8), the eighths of the sky. (Note that, from recent years most stations no longer have cloud detection). We use 5 stability classes based on time of the day and cloud cover data (Table 1). There are also more complex methodologies (cf. e.g. [Mohan and Siddiqui, 1998](#)), but our purpose is to build up a standard methodology that is simple and easy to use. The stability classes have been determined based on the cloudiness data and if the condition is day or night. Daytime hours are defined as the estimated global irradiance from cloud cover above 20 W/m<sup>2</sup> based on the methodology of [Holtslag and Van Ulden \(1983\)](#) and [Popov et al. \(2021\)](#).

Tab. 1: Stability classes, S1 to S5, from unstable to stable

Stability class	day/night, cloud cover [Octa]
S1	day, 0 - 2
S2	day, 3 - 5
S3	day, 6 - 8
S4	night, 5 - 8
S5	night, 0 - 4

The effect of the wind profile on sound propagation depends on the source-receptor line and the angle  $\varphi$  subtended by the wind direction. The crosswind does not affect the sound propagation ( $\cos\varphi = 0$ ). The simplified universal functions used for the calculations ([Defrance et al., 2007](#)) were constructed based on [Businger et al. \(1971\)](#). The shape of the logarithmic term:

$$a_u = \frac{u_* \cos \varphi}{\kappa} \quad (8)$$

The linear term gives the deviation from the logarithmic profile. In the daytime, for unstable stratification ( $T_* < 0$ ,  $L_* < 0$ , Table 2-5):

$$b_u = \frac{u_* \cos \varphi}{\kappa} \frac{1}{L_*} \quad (9)$$

At night-time, with stable stratification ( $T_* > 0$ ,  $L_* > 0$ , Table 2–5):

$$b_u = \frac{u_* \cos \varphi}{\kappa} \frac{4.7}{L_*} \quad (10)$$

Similar principles are used for the constants of the acoustic virtual temperature profile in unstable and stable stratifications:

$$a_c \approx \frac{1}{2} \frac{kR_d}{c_0} 0.74 \frac{T_*}{\kappa} \quad (11)$$

$$b_c \approx \frac{1}{2} \frac{kR_d}{c_0} \left( \frac{T_*}{\kappa} \frac{0.74}{L_*} + \gamma_d \right) \text{ during day} \quad (12)$$

$$b_c \approx \frac{1}{2} \frac{kR_d}{c_0} \left( \frac{T_*}{\kappa} \frac{4.7}{L_*} + \gamma_d \right) \text{ during night} \quad (13)$$

where  $\gamma_d$  [K/m] is dry adiabatic vertical temperature gradient  $\gamma_d=0.0097$  K/m and  $\kappa = 0.4$  is the Von Karman constant.

Tab. 2: Wind speed classes W1 to W5 according to wind speeds at 10 m above the ground and estimated friction velocity ( $u_*$  [m/s])

Wind speed class	V( $z = 10$ m)	$u_*$
W1	0 - 1 m/s	0.00 m/s
W2	1 - 3 m/s	+0.13 m/s
W3	3 - 6 m/s	+0.30 m/s
W4	6 - 10 m/s	+0.53 m/s
W5	>10 m/s	+0.87 m/s

Tab. 3: Temperature scale ( $T_*$  [K]) in different wind speed (W1-W5) and stability classes (S1-S5) classes

	S1	S2	S3	S4	S5
W1	-0.4	-0.2	0	+0.2	0.3
W2	-0.2	-0.1	0	+0.1	0.2
W3	-0.1	-0.05	0	+0.05	0.1
W4	-0.05	0	0	0	0.05
W5	0	0	0	0	0

Tab. 4: Values of  $1/L_*$  [1/m] for different wind speed and stability classes

	S1	S2	S3	S4	S5
W1	-0.08	-0.05	0	+0.04	+0.3
W2	-0.05	-0.02	0	+0.02	+0.2
W3	-0.02	-0.01	0	+0.01	+0.1
W4	-0.01	0	0	0	+0.01
W5	0	0	0	0	0

Tab. 5: The effect of the angle between the sound propagation direction and the wind on sound speed profile calculation

	$u_* \cos \varphi$
V1=-W5	-0.87 m/s
V2=-W4	-0.53
V3=-W3	upwind $V \cos \varphi < -1$ m/s
V4=-W2	-0.13
V5=±W1	crosswind
V6=+W2	+0.13
V7=+W3	downwind $V \cos \varphi > 1$ m/s
V8=+W4	+0.53
V9=+W5	+0.87 m/s

### 2.3 Sound propagation modelling

For us as data providers, it is important to provide the probability of occurrence of downward refraction ( $p_f$ ) and homogeneous ( $1 - p_f$ ) conditions for sound propagation, for the calculation of the noise exposure from a given direction to a fixed receptor point (Fig. 2). In this paper we have calculated the mean, maximum and minimum values of annual  $p_f$  according to the specified period i.e. night (22.00-06.00 h in legal time), day (06.00-18.00 h) and evening (18.00-22.00 h) for Budapest (12843) in period 2009-2018 from hourly meteorological data. Further this annual  $p_f$  values are also calculated for five other cities (Siófok, Pécs, Kecskemét, Szeged and Miskolc) as well as using the ERA5 reanalysis data.

The downward refraction condition is the situation when sound speed increases with height meaning that the gradient of the sound speed is greater than zero:

$$\frac{\partial c}{\partial z} > 0 \quad (14)$$

The homogeneous condition exists when the gradient of sound speed with height decreases or remains constant:

$$\frac{\partial c}{\partial z} \leq 0 \quad (15)$$

The variation of sound speed with height by the derivation of the profile equation (4) is:

$$\frac{\partial c}{\partial z} = \frac{a}{z + z_0} + b \quad (16)$$

Where  $z$  is height above the surface and  $z_0 = 0.1$  m is the roughness length and  $z = 4$  m as per the Hungarian standard,  $a$  and  $b$  are the constants (discrete values) of logarithmic and linear term in the sound speed profile equation. The sound speed gradient is calculated for each hypothetical noise source positioned at 10 degrees around the receptor point according to the wind directions given in the SYNOP reports in each hour of the years. Thus, the gradient of sound speed is calculated for the 36 cases and based on the values of  $a$  and  $b$  (5-5 cases). The 25 possible cases of  $a$  and  $b$  for which sound speed gradient are calculated have been described in Tables 6 and 7. Investigation of  $p_f$  depends from the height is out of our goal. We have analysed the meteorological preprocessor as per the standard version of the Hungarian noise regulation.

Tab. 6: Values of  $a$  in different classes ( $a_1, a_5$ ) based on categories of Tables 3-5

Interval	Discrete value [m/s]
$-\infty < a \leq -0.7$	$a_1 = -1.0$
$-0.7 < a \leq -0.2$	$a_2 = -0.4$
$-0.2 < a \leq +0.2$	$a_3 = 0.0$
$+0.2 < a \leq +0.7$	$a_4 = +0.4$
$+0.7 < a \leq +\infty$	$a_5 = +1.0$

Tab. 7: Values of  $b$  in different classes ( $b_1, b_5$ ) based on categories of Tables 3-5

Interval	Discrete value [1/s]
$-\infty < b \leq -0.08$	$b_1 = -0.12$
$-0.08 < b \leq -0.02$	$b_2 = -0.04$
$-0.02 < b \leq +0.02$	$b_3 = 0.0$
$+0.02 < b \leq +0.08$	$b_4 = +0.04$
$+0.08 < b \leq +\infty$	$b_5 = +0.12$

The selection of the considered height (4 m) was based on the relevant Hungarian legislation (280/2004 (X. 20.) Government Decree). Consideration of different heights indicates a further research direction for us.

The sound levels are calculated based on annual average daily traffic flow data for each vehicle categories ( $m$ ) specified in the CNOSSOS-EU Directive:  $Q_m$  [vehicle/day]. These are multiplied by time factors ( $A_{day}, A_{evening}, A_{night}$ ) that characterize the traffic conditions in Hungary. We obtain the traffic values for each period of day: day (12 hours: 06.00-18.00), evening (4 hours: 18.00-22.00), night (8 hours: 22.00-06.00). Dividing the values by the duration of the given period of day, the average hourly volume of traffic for day, evening and night is calculated  $Q_{m,day}; Q_{m,evening}; Q_{m,night}$  [vehicle/hour]. Additional input data (e.g. speed for each vehicle categories, meteorological data,  $p_f$  parameter) must also to be given for each period of day. Based on these input data, the calculation method provides average sound levels for day, evening and night period:  $L_{day}; L_{evening}; L_{night}$ . According to the Annex I of DIRECTIVE 2002/49/EC, noise indicator  $L_{den}$  is calculated as follows:

$$L_{den} = 10 \times \log \frac{1}{24} \left( 12 \times 10^{\frac{L_{day}}{10}} + 4 \times 10^{\frac{L_{evening}+5}{10}} + 8 \times 10^{\frac{L_{night}+10}{10}} \right) \quad (17)$$

In the previous standard noise propagation methods, the effect of the near-surface air layer was not taken into account with such detail (MSZT, 2002; Krapf and Wetzel, 2005). The later sound propagation models are able to describe the meteorological conditions more accurately (e. g. NMPB 2008 (NF S 31-133, 2011); HARMONOISE (Salomons et al., 2011); VDI (VDI, 2020). In present study, sound propagation model computations were performed using the SoundPLANnoise software version 8.2, (<https://www.soundplan.eu/en/software/soundplannoise/current-version/>), based on the CNOSSOS-EU Road: 2015 calculation method. SoundPLANnoise is an acoustic software with a modular structure, covering a wide range of applications to solve noise calculation, modelling and prediction tasks. The software covers a wide scale of noise types, namely roads, railways, industrial sources (point, line and area sources), indoor and aircraft noise (<https://www.soundplan.eu/>). Among display options there are tables, façade or grid noise maps, presentation of noise load at immission points and 3D visualisation ([https://vibrocomp.hu/soundplan](https://vibrocomp.hu/soundplan;); Ozkurt, 2014). On the study area, the sound levels for day, evening and night period ( $L_{day}$  [dB(A)],  $L_{evening}$  [dB(A)],  $L_{night}$  [dB(A)], respectively) were calculated at the receiver points.  $p_f$  values as input data of the model can be provided as a single value or with one value for each 20° sector for each period of the day.

### 3 DATASET AND STUDY AREA

The hourly synoptic datasets of HMS were downloaded from the Meteomanz and Ogimet websites for those years when cloud measurements were available. The amount of cloud cover is given in octas (0, 1, ..., 8), the eighths of the sky. (Note that, from recent years most stations no longer have cloud detection).

Hourly observations in Budapest (12843) for the 10-year period of 2009-2018 are analysed. We are also using out the data from five additional synoptic stations for 2014-2018, to get an idea of the differences of  $p_f$ , probability of occurrence of downward refraction conditions within the country. These examined measurement sites are: Siófok, Pécs, Kecskemét, Szeged and Miskolc. The applicability of gridded datasets (here ERA5) is analysed at the closest grid cell to the Pestszentlőrinc, (12843) HMS station for the year-2014.

The quality control of the downloaded SYNOP databases was accomplished by filling in missing data. In cases of short data gaps (up to 6 measurement cycles missing), linear interpolation was used, while for longer data gaps, the gap-filling was performed based on the data of the previous and the following 1-3 days, leaving a maximum of 3 hours of adjustment time to fit the measured and interpolated data. The missing data in the year were between 0.1-1.5%.

The study area shown in Fig. 3-4 is located in the Municipality of Üllő, which is a town in Pest County, Hungary. The location is approximately 13 km from Pestszentlőrinc (12843) HMS station. The study area is crossed by Highway 4, which is a major road according to the 49/2002 EU Directive, as it has more than three million vehicle passages a year on the examined section. In site selection, it was a main aspect that on the left side of the road there is no obstacles (e.g. buildings, barriers) which would influence the sound propagation. 41 receiver points were designated in increasing distance from Highway 4 as road traffic emission source.

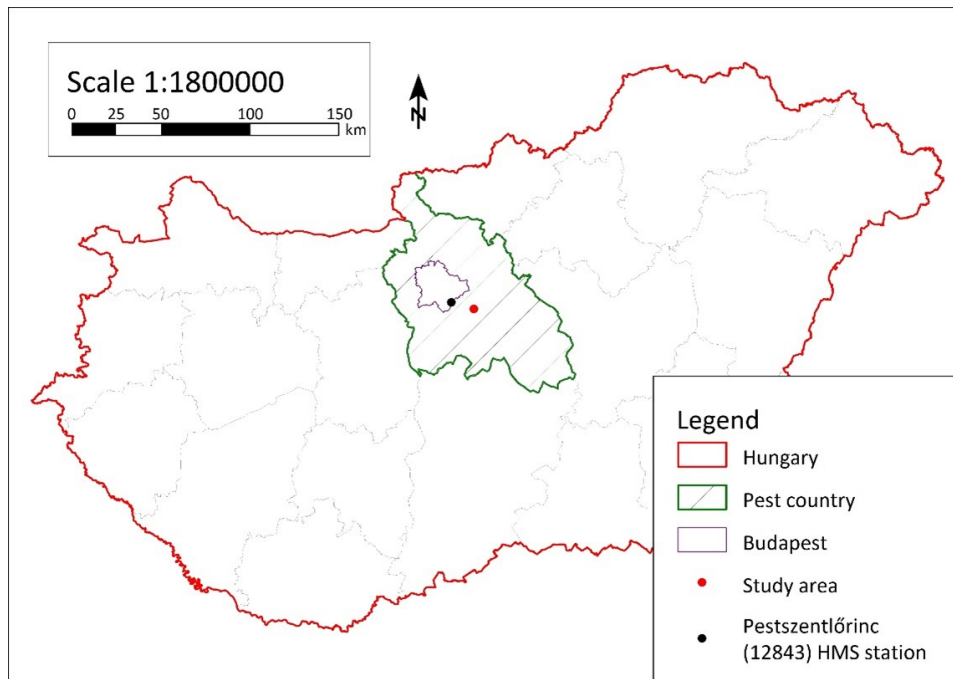


Fig. 3: Location of the study area

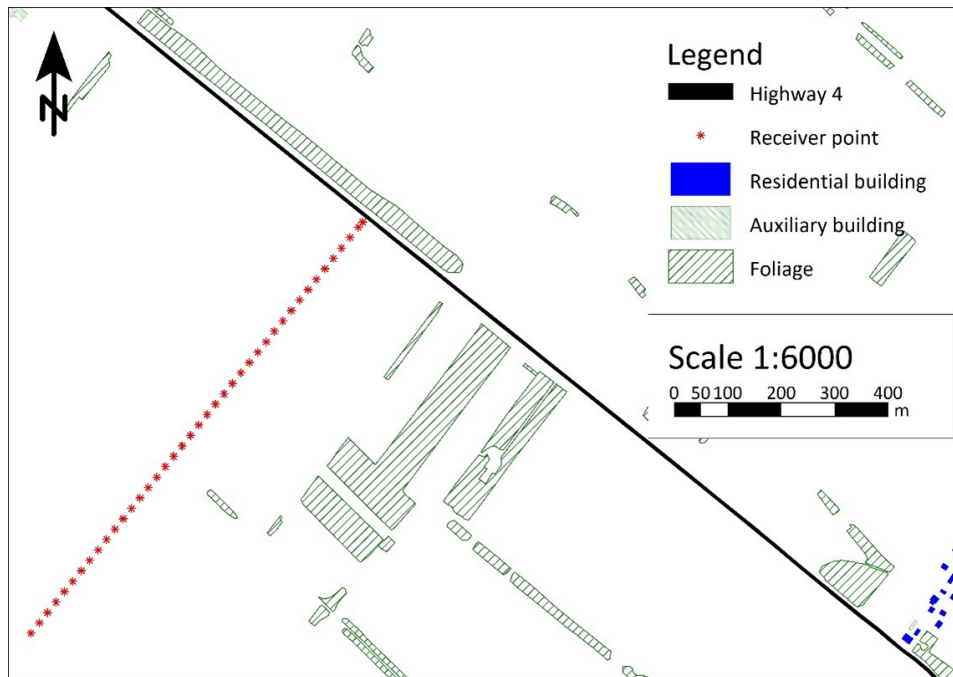


Fig. 4: Structure of the study area

Road traffic noise emission was determined applying the CNOSSOS-EU calculation method, based on the 2021 annual average daily traffic flow data. Public cross-sectional flow data in 2021 for the examined road section of Highway 4 were downloaded from the website of Hungarian Public Roads. The emission sound power levels in each period of the day are  $L_{w,day} = 87.2$  dB(A),  $L_{w,evening} = 85.2$  dB(A) and  $L_{w,night} = 81.8$  dB(A). According to the traffic regulation for that given road section, the speed limit was considered as 90 km/h for light motor vehicles and motorcycles, and 70 km/h for medium heavy and heavy vehicles. The digital terrain model, the foliage dataset and the road geometry data were provided from the input data used in the latest round of strategic noise mapping in Hungary.

### 4 RESULTS AND DISCUSSION

First of all, we looked at the 10-year data series for Budapest. In 34% of cases, the daytime – between 06.00-18.00 hrs – was the most favourable (downward refraction) period for noise propagation. In the evening, it is mostly stable between 18.00-22.00 hrs, and at night, between 22.00-06.00 hrs 59% and 64% respectively. There is a surprisingly high number of indifferent ( $a = 0, b = 0$ ) sound speed profiles, ranging from 15-35% depending on the time of the day and receptor point orientation. Based on the results a recommendation can be made to introduce a third quasi-indifferent profile category into the meteorological preprocessor.

Next, we analysed the relative frequencies of the 25 stability categories ( $a_1$ - $a_5, b_1$ - $b_5$ ). Out of the 25 possible classes, only 11 have an occurrence rate (Fig. 5). This is understandable since, e.g., at high wind speeds, highly unstable stratification cannot develop. In this case, stratification is close to indifferent. During the daytime, we are more likely to see homogeneous sound propagation, while during the evening and night-time, the speed of sound increases with height in most cases (downward refraction). If we look at the differences between years, e.g., for indifferent cases, ( $a = 0, b = 0$ ), the relative standard deviation (% of standard deviation/expected value) is around 5% in all three periods of the day. These are small values. Large relative standard deviations (>15-20%) are usually found in cases of strong upwind and downwind situations, but the number of cases is small. In weak upwind and downwind situations (with high case rates), the standard deviations are between 10-20%. (These are low wind and crosswind situations).

The variation of the sound speed with height ( $\frac{\partial c}{\partial z}$ ) was calculated at  $z = 4$  m height. Considering i) the downward refraction ( $100p_f$  [%]), ii) the homogeneous conditions ( $(100(1-p_f))$  [%]) and iii) the frequency of indifferent ( $a = 0, b = 0$ ) situations which we classify as a subcategory within the homogeneous conditions group in the case of the two-category classification (Fig. 6). The highest number of downward refraction situations (potentially high noise exposure) is found in the northwest/northeast sector. This is understandable because this is the most common wind direction in the region (Radics and Bartholy, 2008).

The highest number of homogeneous cases is found on the opposite side. (Our “wind rose” in Figure 6 shows the frequency of cases (in %) depending on the location of the 36 virtual noise sources). The probability of indifferent cases is high. During daytime hours, the values perpendicular to the main wind direction, together with light crosswind situations, exceed 35%. As expected, the asymmetric distribution of homogeneous and downward refraction situations is visible. In the evening and night periods, the difference between the frequencies of each direction is smaller than during the day.

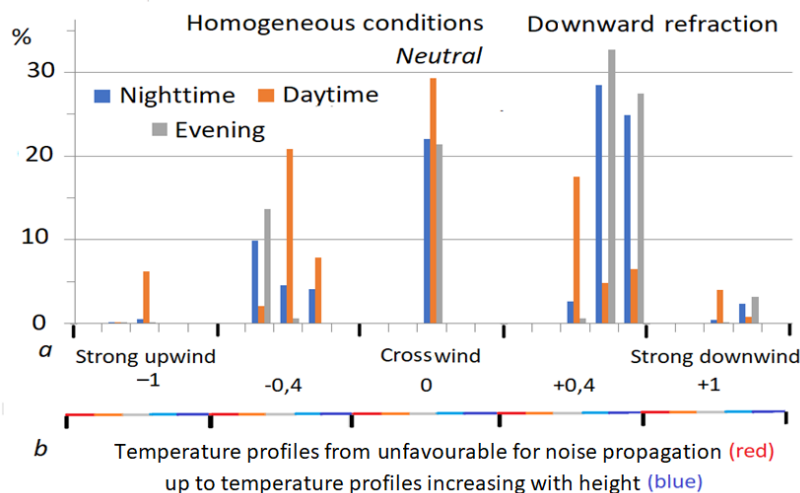


Fig. 5: Relative frequency [%] of noise propagation in the 25 stability classes based on the hourly dataset (from 2009 to 2018) for Budapest (12843). Increasing values of  $a$  (logarithmic term) indicate increased with stability and/or wind speed in the direction of noise propagation while increasing values  $b$  (linear term) indicate stability (from unstable to stable stratification) and the current wind profile.

The standard deviations of the annual frequencies for each direction are small, between 1-5%, based on the 10-year Budapest data series. Finally, we examined the differences between the highest and lowest annual relative frequencies [%] as well as the mean values of annual relative frequencies [%] in each direction for the downward refraction situations. The results for day, evening and night periods are presented in (Fig. 7-9), respectively. For day period, the most significant differences between minimum and maximum values are around 15% in the sectors that are perpendicular to the main wind direction. The smallest absolute deviations are in the north and south directions, with values of around 5%. The highest maximum  $p_f$  values occur in the evening period.

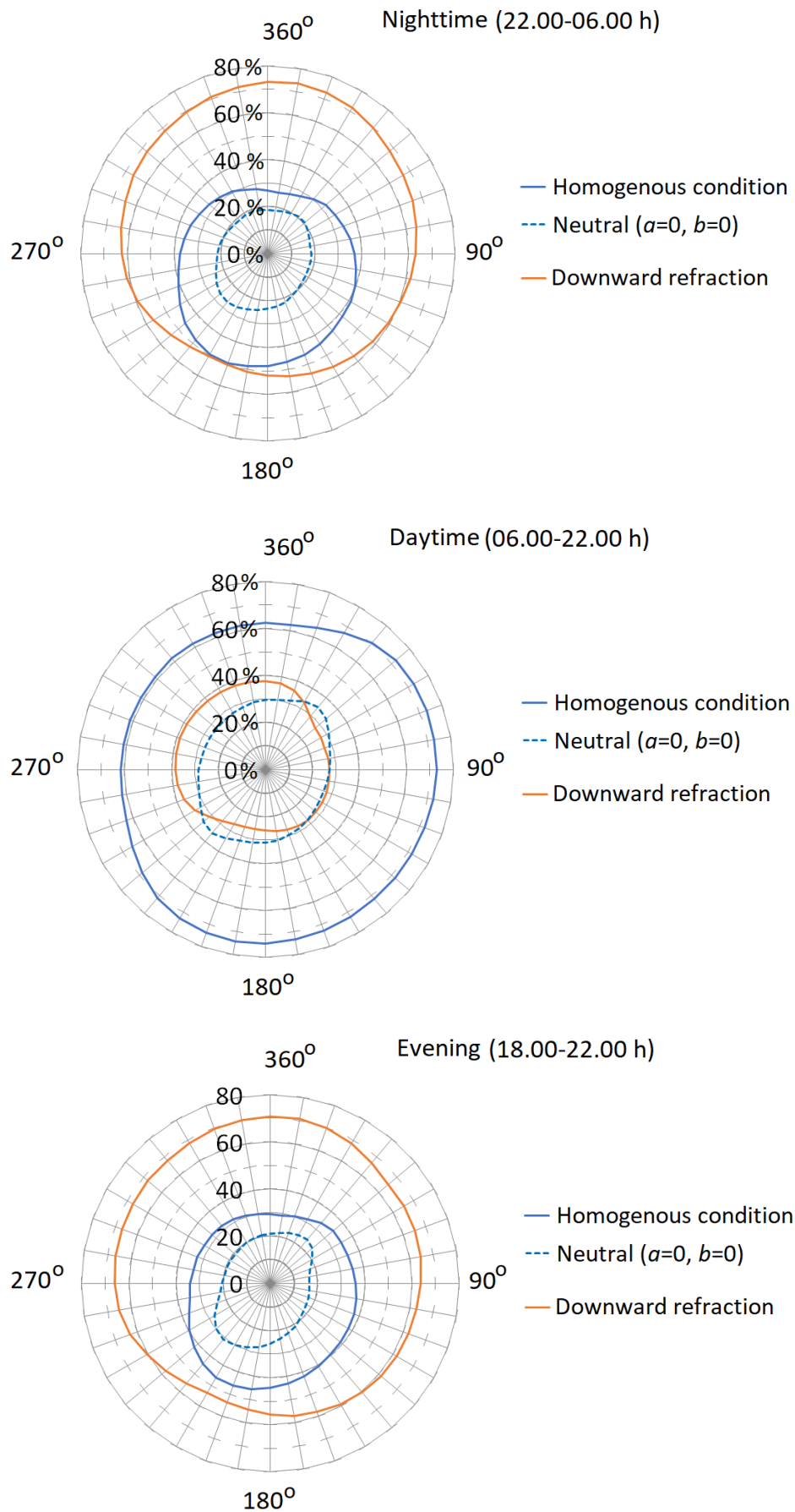


Fig. 6: Noise pollution for homogeneous condition, downward refraction cases, and indifferent stratification (a subcategory of homogeneous condition) for night-time, daytime, and evening in legal time (Budapest, 2009-2018)

In the case of wind blowing from the 270-360° sector, the 10-year maximum  $p_f$  values reach 80%. The smallest value occurs in the opposite sector. The night period shows a similar shape, but it can be characterized by smaller maximum values. This is explained by the daily course of the wind speed and the stable air stratification. In the evening and night hours, an inversion situation usually develops. This is accompanied by the evening wind speed minimum, which causes downward refraction situations (potentially high noise exposure) in weak downwind situations in addition to inversion temperature stratification. The largest differences between the highest and lowest annual  $p_f$  values occur in the evening hours. That is understandable, since during the evening period, the ratio of stable and unstable stratification which are close to the indifferent one can change significantly among the years (transitional stratification). This significant difference will be reflected in the noise propagation calculation results as well. In addition to the 10-year Budapest dataset, we also analysed the average relative frequencies of probability  $p_f$  in all three time periods based on hourly data from 5 other SYNOP stations in Hungary for years between 2014 and 2018 (Fig. 10). The difference between  $p_f$  values is less than 2% for the two 5-year periods in Budapest for each time period of the day. The variance within the two 5-year periods is less than 1% in the daytime, but not more than 2% in the other two periods. Thus, it is sufficient to work with 5-year data series.

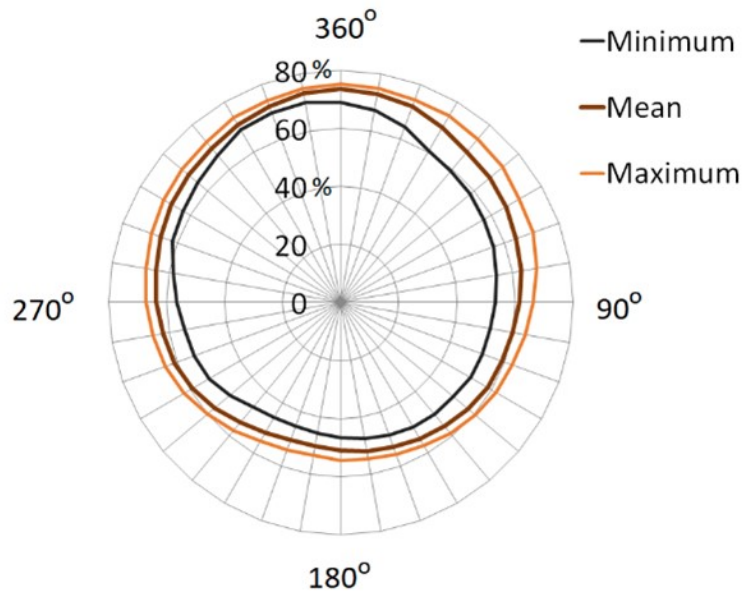


Fig. 7: Minimum, maximum and mean annual frequencies (in %) of downward refraction cases for noise pollution for 10 years (2009-2018), based on the hourly data during the night period (Budapest, 12843).

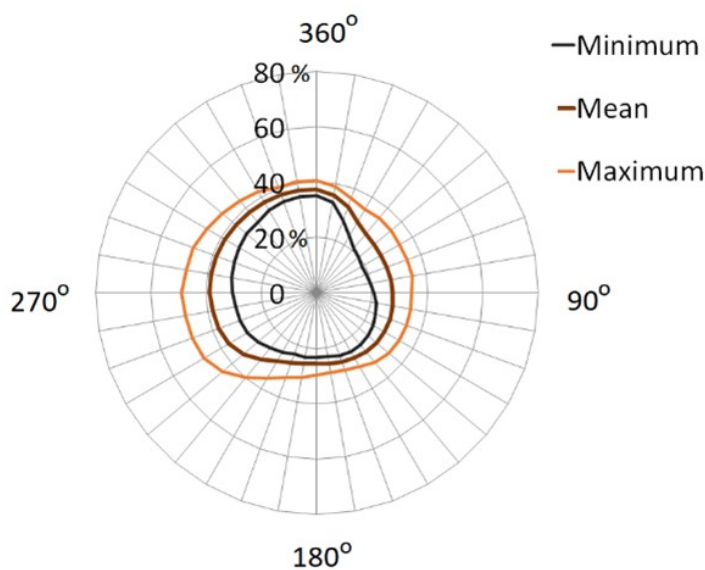


Fig. 8: Minimum, maximum and mean annual frequencies (in %) of downward refraction cases for noise pollution for 10 years (2009-2018), based on the hourly data during the day period (Budapest, 12843).

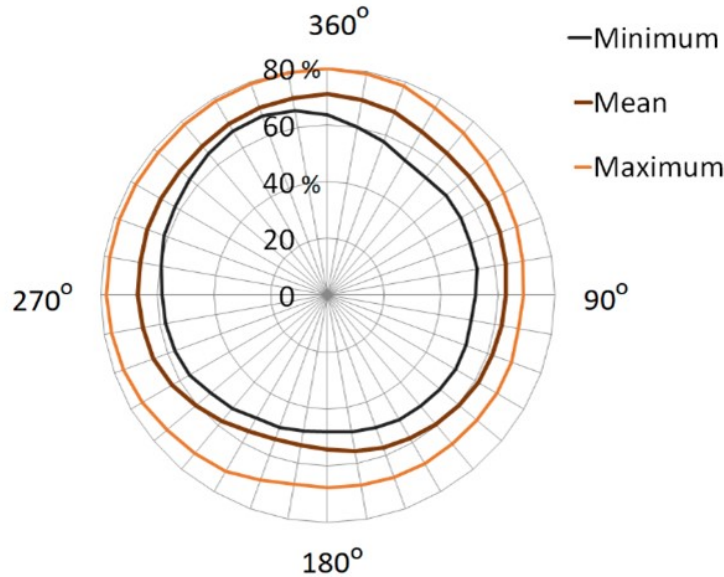


Fig. 9: Minimum, maximum and mean annual frequencies (in %) of downward refraction cases for noise pollution for 10 years (2009-2018), based on the hourly data during the evening period (Budapest, 12843).

The results from Budapest and the four rural cities (except Miskolc) provide similar characteristics. The 5-year averages show differences of a few per cent ( $\leq 5\%$ ). However, the evening and night  $p_f$  values for Miskolc are significantly higher than those of the other stations, by more than 20%. This is because of many unfavourable cases. The station is located in a valley outside the city. Low wind speeds are the first of the explanatory factors. The average value of wind speed is around 1.5 m/s is nearly half of the average in Hungary (2.5-3.5 m/s). During the daytime, however, there are no major differences compared to other stations. Moreover, the applicability of the ERA5 database (Hersbach et al., 2020) in noise propagation tasks was analysed. The data of the nearest grid point to the Pestszentlőrinc (12843) station were processed. Our results for the year 2014 are shown in Table 8. Thus, we can compare the probability ( $p_f$ ) data based on i) directly calculated from the measured data (SYNOP, 12843), ii) the hourly meteorological data (ERA5 MET) and iii) turbulence characteristics ( $u_*$ ,  $T_*$ ,  $L_*$ ) from the ERA5 reanalysis dataset (ERA5 flux). Significant differences are found between  $p_f$  values calculated using measured and reanalysed meteorological data especially in the evening and in the night period, while the day values show a surprising similarity. The  $p_f$  data calculated from the measured values and ERA5 turbulence characteristics show a strong agreement at all three times of the day. Differences are below 3%. Further analysis is required for a more detailed explanation. In any case, it can be concluded that the ERA5 database has “suitable room” for further investigation.

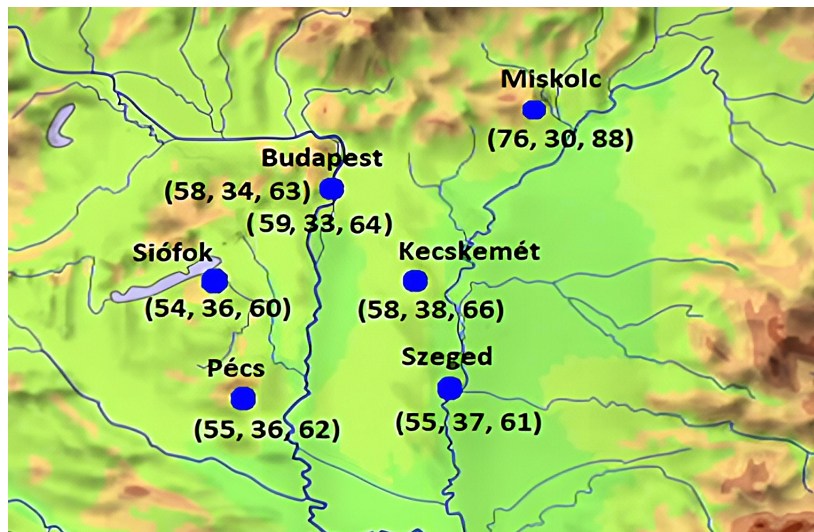


Fig. 10: Relative frequencies ( $p_f$  [%]) of downward refraction cases for two 5-year periods for Budapest (2009-2013, top) and 2014-2018, bottom) and for five other Hungarian cities in the Pannonian Basin (2014-2018). The values in parentheses represent the night, day, and evening periods, respectively.

For the sound propagation model calculations, the following five versions of the input dataset of the parameter  $p_f$  were applied

- *pmín*: the lowest annual relative frequencies (%) for the downward refraction situations in each direction, for each period of the day, based on the 10-year Budapest data series, as provided above ((Fig. 7-9), minimum values),

Tab. 8: Measured and calculated  $p_f$  values from the ERA5 database for the Budapest grid point based on hourly data for three time periods in 2014

Data source	Night	Day	Evening
SYNOP	59%	33%	65%
ERA5 met	48%	35%	51%
ERA5 flux	58%	36%	68%

- $p_{max}$ : the highest annual relative frequencies (%) for the downward refraction situations in each direction, for each period of the day, based on the 10-year Budapest data series, as provided above ((Fig. 7-9), maximum values),
- $p_{mean}$ : the mean annual relative frequencies (%) for the downward refraction situations in each direction, for each period of the day, based on the 10-year Budapest data series, as provided above ((Fig. 7-9), mean values),
- $p_{BUB}$ :  $p_f = 50\%$  for the day period;  $p_f = 75\%$  for the evening period;  $p_f = 100\%$  for night period, as recommended by the German implementation of CNOSSOS-EU (BUB) (Moehler et al., 2006; Kephelopoulos et al., 2012; Brannolte et al., 2021),
- $p1$ :  $p_f = 100\%$  for each period of the day, as a “worst-case scenario”.

The results of the model calculations are shown in (Fig. 11-13) for the day, evening and night periods, respectively. The sound pressure levels are indicated as a function of the distance from the source. The distance of the first receiver point from the source is 12.5 m, and the furthest one is 1000 m. Close to the source, the sound pressure levels calculated using the different versions of parameters are quite similar (at the first receiver point, the sound pressure levels are 71.0-71.3 dB(A), 69.4-69.5 dB(A), 65.6-65.8 dB(A) for the day, evening and night period, respectively), since the effect of the deviation in the values of the parameter  $p_f$  is not shown yet. The deviation between the different version begin to increase after 50 m. In general, it can be said that the attenuation of sound pressure levels with distance is greater during the turbulence and smaller  $p_f$  values. Where the value of  $p_f$  is the same in each period of the day (version  $p1$ ), also the degree of attenuation with distance is almost the same at each time of the day, only minimally higher during daytime. Comparing the results based on the highest and lowest annual relative frequencies determined based on the 10-year Budapest data series versions ( $p_{min}$ ) and ( $p_{max}$ ), it can be established that larger differences in sound levels can be detected during the day and evening period (the maximum values of deviations are 1.65 dB(A) and 1.42 dB(A), respectively), while in the night period there are lower differences (with a maximum value of 0.75 dB(A). This may be explained by the fact that the ( $p_{min}$ ) and ( $p_{max}$ ) values themselves show a smaller difference during the night period than in the other periods. This is because of the location of the source and the receiver points, which causes downwind cases to occur more often. As expected, the worst-case scenario of  $p_f$  values resulted in significantly higher sound levels compared to the other versions (the maximum differences can exceed even 5 dB(A) for the day). An exception is the ( $p_{BUB}$ ) version for the night period, where the  $p_f$  value was the same as in the worst-case scenario ( $p_f = 1$ ). The sound levels calculated with the  $p_f$  values of ( $p_{BUB}$ ) version are higher than those counted with the  $p_f$  values generated by the developed preprocessor not only for the night period but also for the daytime. This may be due to the decision that indifferent cases were classified as homogeneous cases in our method. However, the results for the evening period calculated with  $p_f$  values of ( $p_{BUB}$ ) and ( $p_{max}$ ) versions are very similar. This is because the generated values of ( $p_{max}$ ) version and the values according to the German standard ( $p_{BUB} = 75\%$ ) are close to each other in the evening hours. To sum up, it can be stated that the parameter  $p_f$  can have a considerable effect on CNOSSOS-EU sound propagation model outputs. Therefore, it is a very important issue to determine the values of the parameter  $p_f$  in a well-established way, taking into account the local meteorological conditions as well.

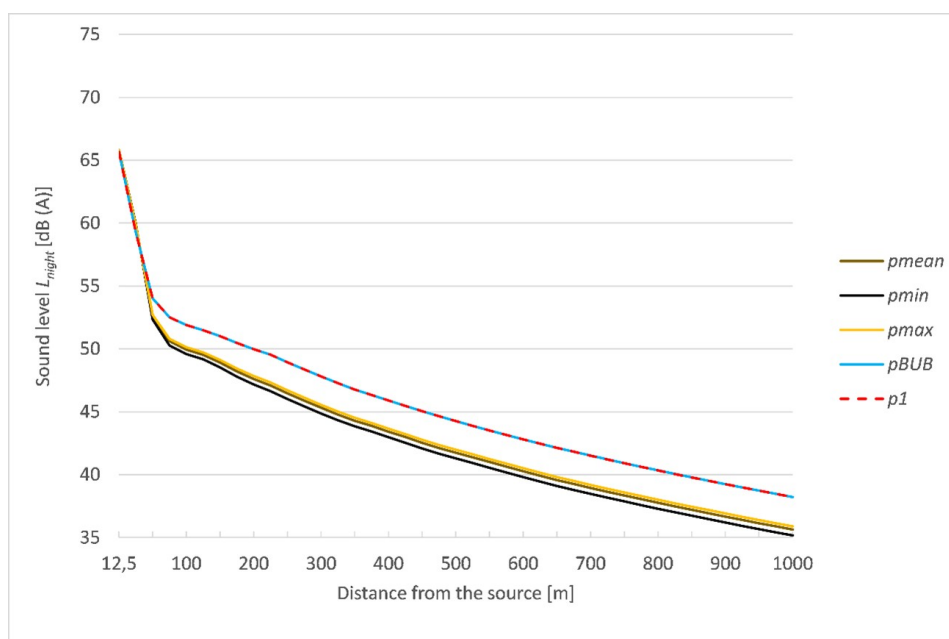


Fig. 11: Sound levels for the night period as a function of the distance from the source for each version of the input dataset of parameter  $p_f$

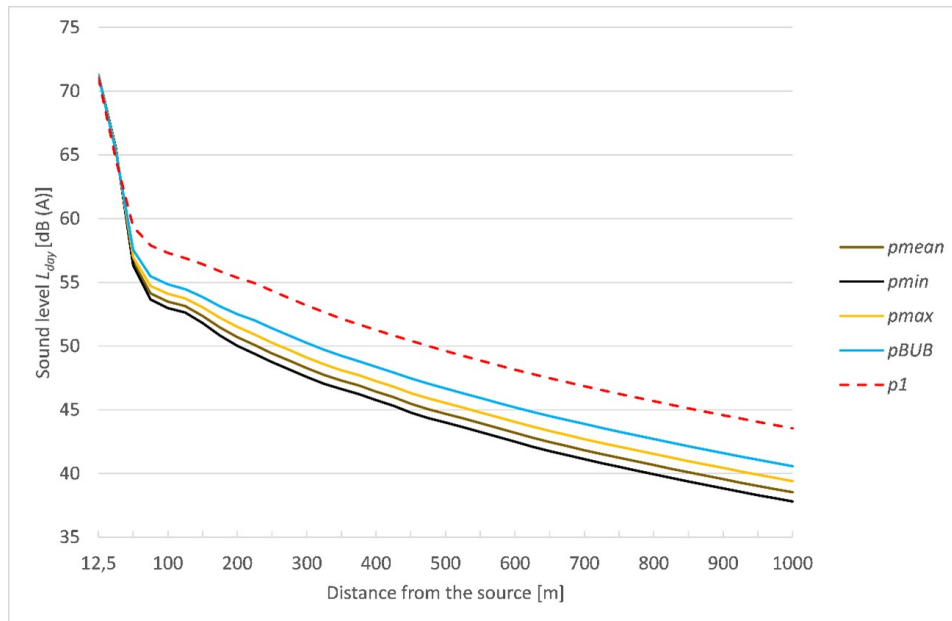


Fig. 12: Sound levels for the day period as a function of the distance from the source version of the input dataset of parameter  $p_f$

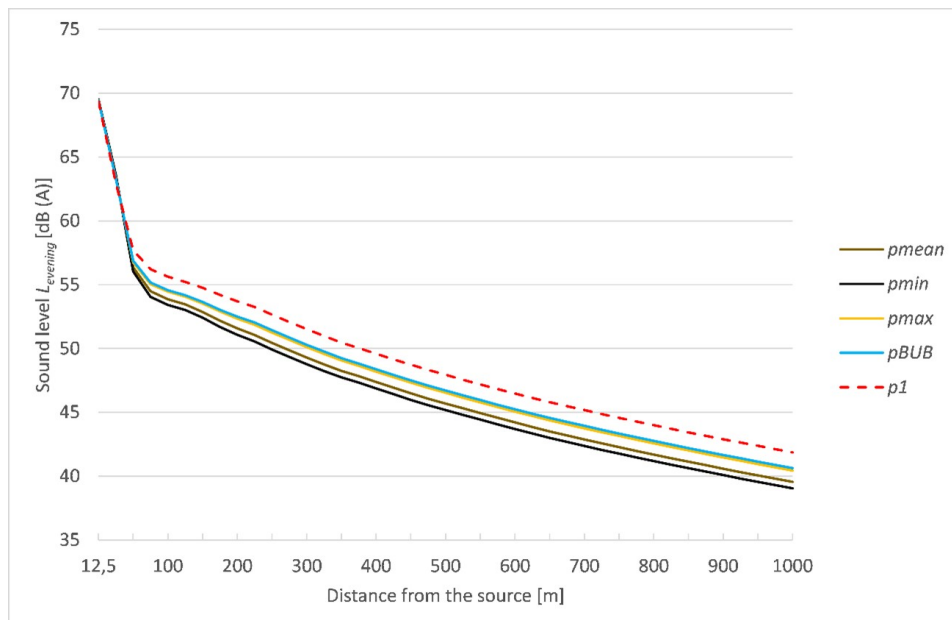


Fig. 13: Sound levels for the evening period as a function of the distance from the source for each version of the input dataset of parameter  $p_f$

## 5 SUMMARY

A meteorological preprocessor was developed for the noise propagation model of the CNOSSOS-EU method to separate homogeneous conditions and downward refraction noise propagation situations for different times of the day based on the atmospheric stability, temperature, wind speed and direction data. A virtual noise source was placed around the imaginary receptor point every 10 degrees. Our main conclusions from the investigation of a 10-year dataset for Budapest (12843) are:

- Strong upwinds ( $a = -1$ ) and downwinds ( $a = +1$ ) are most frequent in the main wind directions (NW, SE), while slow winds ( $a = 0, 4$ ) are generally 30-60 degrees different, while light and crosswinds ( $a = 0$ ) are most frequent in perpendicular to the main wind direction.
- High winds are more frequent during the day.
- The directional distribution of the up- and downwind cases is almost a mirror image of each other.
- As expected, the most downward refraction situations for propagation occur in the evening and at night in about 2/3 of the cases, and during the day in about 1/3 of the cases.

Analyses of data from five other Hungarian weather stations, except Miskolc, show the general features. The station at Miskolc is in a valley represented by low wind speed, which does not give representative results. There were few variations among other stations. There is also a moderate variability in the  $p_f$  probability values among years (few %).

The ERA5 reanalysis dataset can be successfully used to build a noise propagation meteorological preprocessor. However, significant differences are found between the meteorological reanalysis data and the computations based on the ERA5-derived turbulence parameters. Using i) more stations and ii) grid cells from the ERA5 provides a sensitivity analysis of the preprocessor based on a different set of universal functions, which is also an important goal for the near future. The main conclusion from the sound propagation model calculations is that there is a significant difference in the sound levels calculated using the  $p_f$  values generated taking into account the local meteorological conditions and those counted using the  $p_f$  values according to the worst-case scenario ( $p_f = 1$  for each period of the day) or a recommendation of another Member State ( $p_f = 0.5; 0.75; 1$  for day, evening and night period, respectively). These results underline the importance of a well-established determination of the parameter  $p_f$ , taking into account the local meteorological conditions.

Further research objectives include:

- a sensitivity study of noise propagation meteorological preprocessor using different types of universal functions,
- the development of a grid point database for the probability of occurrence of downward refraction conditions ( $p_f$ ) in Hungary based on long-term meteorological measurements and ERA5 reanalysis.

## Acknowledgement

The authors would like to thank Viola Parászka and Regina Blumberger of the KTI Institute for Transport Sciences Non-profit Ltd. for their assistance and useful comments. They would also like to thank Peter K. Musyimi, who proofread and checked the grammar. This work has been funded by the Ministry of Technology and Industry under contract GVF/337/2021-ITM-SZERZ and by the Hungarian National Research, Development, and Innovation Centre under contract No. K-138176.

## References

- P.S. Arya. *Introduction to micrometeorology*. 2nd Edition, Elsevier, 2001. doi: [ISBN 9780080489261](https://doi.org/10.1016/B978-0-08-048926-1).
- K. Attenborough. Sound propagation in the atmosphere. In *Springer Handbook of Acoustics*, pages 117–155. Springer, 2014. doi: [doi: 10.1007/978-1-4939-0755-7\\_4](https://doi.org/10.1007/978-1-4939-0755-7_4).
- E.A. Balogh, T. Schmelz, and L. Orosz. Sensitivity of CNOSSOS-EU sound propagation model to digital surface components. *Acta Technica Jaurinensis*, 15(1):47–57, 2022. doi: [10.14513/actatechjaur.00644](https://doi.org/10.14513/actatechjaur.00644).
- U. Brannolte, R. Harder, C. Walther, T. Schäfer, and A. Dahl. Bekanntmachung der Vorläufigen Berechnungsverfahren für den Umgebungslärm nach § 5 Abs. 1 der Verordnung über die Lärmkartierung (34. BImSchV). In *Stadtverkehrsplanung Band 2*, pages 161–206. Springer, 2021. doi: [BAnz AT 05.10.2021 B4](https://doi.org/10.1007/978-3-7089-1444-4_4).
- J.A. Businger, J.C. Wyngaard, Y. Izumi, and F. Bradley. Flux-profile relationships in the atmospheric surface layer. *Journal of Atmospheric Sciences*, 28(2):181–189, 1971. doi: [10.1175/1520-0469\(1971\)028<0181:FPRITA>2.0.CO;2](https://doi.org/10.1175/1520-0469(1971)028<0181:FPRITA>2.0.CO;2).
- J. Deepak. Noise pollution: A review. *Journal of Environment Pollution and Human Health*, 4(3):72–77, 2016. doi: [10.12691/jephh-4-3-3](https://doi.org/10.12691/jephh-4-3-3).
- J. Defrance, E. Salomons, I. Noordhoek, D. Heimann, P. Birger, G. Watts, H. Jonasson, X. Zhang, E. Premat, I. Schmich, M. Aballea, M. Baulac, and F. Roo. Outdoor sound propagation reference model developed in the European harmonoise project. *Acta Acustica united with Acustica*, 93(2):213–227, 2007. doi: [Hirtzel. ISSN 1610-1928. Volltext nicht online](https://doi.org/10.1052/1.1511111).
- Directive 2002/49/EC. 2002/49/EC of the European Parliament and of The Council of 25 June 2002 relating to the assessment and management of environmental noise. *Official Journal of the European Communities*, L 189/12:12–26, 2002. doi: [Document 32002L0049](https://doi.org/10.1052/1.1511111).
- Directive 2015/996/EU. Commission (EU) 2015/996 of 19 May 2015 establishing common noise assessment methods according to directive 2002/49/ec of the European Parliament and of the Council (Text with EEA relevance). *Official Journal of the European Union*, L 168:1–823, 2015. doi: [Document 32015L0996](https://doi.org/10.1052/1.1511111).
- G. Dutilleul, J. Defrance, F. Junker, D. Ecotière, B. Gauvreau, D. van Maercke, E. Le Duc, M. Bérengier, and F. Besnard. *Road noise prediction 2 - Noise propagation computation method including meteorological effects (NMPB 2008)*. 142 p. Sétra authorisation is strictly required for even partial reproduction of this document. Reference : 0957-2A, 2009.
- R. Eurasto. *NORD2000 for road traffic noise prediction WP4. Weather classes and statistics*. Technical Report VTT-R-02530-06, VIT Technical Research Center of Finland, 2006.
- J.-P. Faulkner, E. Murphy, H.J. Rice, and J. Kennedy. Towards a Good Practice Guide for Implementing CNOSSOS-EU in Ireland. Technical report, EPA RESEARCH PROGRAMME 2021–2030. *Published by Environmental Protection Agency, Wexford, Ireland*, 2021.
- S. Fiorino, S. Bose-Pillai, and K. Keefer. Re-visiting acoustic sounding to advance the measurement of optical turbulence. *Applied Sciences*, 11(16):7658, 2021. doi: [10.3390/app11167658](https://doi.org/10.3390/app11167658).
- T. Foken. *Micrometeorology*. Second Edition, Springer Nature, 2017. doi: [doi: 10.1007/978-3-642-25440-6](https://doi.org/10.1007/978-3-642-25440-6).
- S.L. Garrett. Reflection, transmission, and refraction. In *Understanding Acoustics. Graduate Texts in Physics*. Springer, 2020. (eBook), pages 513–542. Springer, 2020. doi: [org/10.1007/978-3-030-44787-8](https://doi.org/10.1007/978-3-030-44787-8).
- R. Guski, D. Schreckenber, and R. Schuemer. WHO Environmental Noise Guidelines for the European Region: A Systematic Review on Environmental Noise and Annoyance. *International Journal of Environmental Research and Public Health*, 14(12): 1539, 2017. doi: [10.3390/ijerph14121539](https://doi.org/10.3390/ijerph14121539).

- H. Hersbach, B. Bell, P. Berrisford, S. Hirahara, A. Horányi, J. Muñoz-Sabater, J. Nicolas, C. Peubey, R. Radu, D. Schepers, A. Simmons, C. Soci, S. Abdalla, X. Abellan, G. Balsamo, P. Bechtold, G. Biavati, J. Bidlot, M. Bonavita, G. De Chiara, P. Dahlgren, D. Dee, M. Diamantakis, R. Dragani, J. Flemming, R. Forbes, M. Fuentes, A. Geer, L. Haimberger, S. Healy, R.J. Hogan, E. Hólm, M. Janisková, S. Keeley, P. Laloyaux, P. Lopez, C. Lupu, G. Radnoti, P. de Rosnay, I. Rozum, F. Vamborg, S. Villaume, and J.-N. Thépaut. The ERA5 global reanalysis. *Quarterly Journal of the Royal Meteorological Society*, 146(730): 1999–2049, 2020. doi: [10.1002/qj.3803](https://doi.org/10.1002/qj.3803).
- A.A.M. Holtslag and A.P. Van Ulden. A simple scheme for daytime estimates of the surface fluxes from routine weather data. *Journal of Applied Meteorology and Climatology*, 22(4):517–529, 1983. doi: [10.1175/1520-0450\(1983\)022<0517:ASSFDE>2.0.CO;2](https://doi.org/10.1175/1520-0450(1983)022<0517:ASSFDE>2.0.CO;2).
- S. Kephelopoulos, M. Paviotti, and F. Anfosso-Lédée. *Common noise assessment methods in Europe (CNOSSOS-EU)*. Publications Office of the European Union, January 2012. doi: [10.2788/31776](https://doi.org/10.2788/31776). URL <https://hal.science/hal-00985998>.
- S. Khomenko, M. Cirach, J. Barrera-Gómez, E. Pereira-Barboza, T. Iungman, N. Mueller, M. Foraster, C. Tonne, M. Thondoo, C. Jephcote, J. Gulliver, J. Woodcock, and M. Nieuwenhuijsen. Impact of road traffic noise on annoyance and preventable mortality in European cities: A health impact assessment. *Environment International*, 162:107160, 2022. doi: [10.1016/j.envint.2022.107160](https://doi.org/10.1016/j.envint.2022.107160). Epub 2022 Feb 26. PMID: 35231841.
- G. Krapf and E. Wetzel. Adaptation of national noise prediction methods to directive 2002/49/EC requirements on noise mapping. In *Forum Acusticum Conference*, pages 995–998, 2005.
- P. Majjala and O. Kontkanen. CNOSSOS-EU sensitivity to meteorological and to some road initial value changes. In *INTER-NOISE and NOISE-CON Congress and Conference Proceedings*, volume 253, pages 6245–6256. Institute of Noise Control Engineering, 2016. URL <http://pub.dega-akustik.de/IN2016/data/articles/000880.pdf>.
- U. Moehler, M. Liepert, U.J. Kurze, and H. Onnich. The new German Prediction model for railway noise "schall 03 2006" - Some proposals for the harmonised calculation method in the EU directive on environmental noise. *Proceedings of Eronoise*. 2006. doi: [10.1007/978-3-540-74893-9\\_26](https://doi.org/10.1007/978-3-540-74893-9_26).
- M. Mohan and T.A. Siddiqui. Analysis of various schemes for the estimation of atmospheric stability classification. *Atmospheric Environment*, 32(21):3775–3781, 1998. doi: [10.1016/S1352-2310\(98\)00109-5](https://doi.org/10.1016/S1352-2310(98)00109-5).
- MSZT. Outdoor sound propagation (msz 15036) (In Hung.). *Hungarian Standards Institution (MSZT)*, 2002.
- NF S 31-133. Acoustics — outdoor noise — calculation of sound levels, 2011.
- V.E. Ostashev and D.K. Wilson. *Acoustics in moving inhomogeneous media*. London CRC Press, 2015. doi: [10.1201/b18922](https://doi.org/10.1201/b18922).
- N. Ozkurt. Current assessment and future projections of noise pollution at Ankara Esenboğa Airport, Turkey. *Transportation Research Part D: Transport and Environment*, 32:120–128, 2014. doi: [doi: 10.1016/j.trd.2014.07.011](https://doi.org/10.1016/j.trd.2014.07.011).
- E. Peris. (lead author) Environmental noise in Europe: 2020. *EEA Report No 22/2019*, European Environment Agency, 1:104, 2020. doi: [10.2800/686249](https://doi.org/10.2800/686249).
- Z. Popov, Z. Nagy, G. Baranka, and T. Weidinger. Assessments of solar, thermal and net irradiance from simple solar geometry and routine meteorological measurements in the Pannonian Basin. *Atmosphere*, 12(8):935, 2021. doi: [10.3390/atmos12080935](https://doi.org/10.3390/atmos12080935).
- K. Radics and J. Bartholy. Estimating and modelling the wind resource of Hungary. *Renewable and Sustainable Energy Reviews*, 12(3):874–882, 2008. doi: [doi: 10.1016/j.rser.2006.10.009](https://doi.org/10.1016/j.rser.2006.10.009).
- E. Salomons, D. Van Maercke, J. Defrance, and F. de Roo. The Harmonoise sound propagation model. *Acta acustica united with acustica*, 97(1):62–74, 2011. doi: [10.3813/AAA.918387](https://doi.org/10.3813/AAA.918387).
- A.A. Tsonis. *An introduction to atmospheric thermodynamics*. Cambridge University Press, 2 edition, 2007. doi: [10.1017/CBO9780511619175](https://doi.org/10.1017/CBO9780511619175).
- VDI. *Schallausbreitung im Freien*. VDI 2714 Beuth-Verlag, Berlin, 1988. DIN ISO 9613-2:1999-10.
- VDI. Blatt 1 – Draft, *Sound propagation outdoors in consideration of meteorological and topographical conditions - part 1: phenomena and Procedures*, 2020.
- T. Weidinger, J. Pinto, and L. Horváth. Effects of uncertainties in universal functions, roughness length, and displacement height on the calculation of surface layer fluxes. *Meteorologische Zeitschrift*, 9(3):139–154, 2000. doi: [10.1127/metz/9/2000/139](https://doi.org/10.1127/metz/9/2000/139).
- WHO. *WHO environmental noise guidelines for the European Region*, 2018. URL <https://www.euro.who.int/en/health-topics/environment-and-health/noise/environmental-noise-guidelines-for-the-european-region>.